PNAS

Subchronic elevation in ambient temperature drives alterations to the sperm epigenome and accelerates early embryonic development in mice

Natalie Trigg[a,b,c,d,e,f], John E. Schjenken[a,b,1], Jacinta H. Martin[a,b], David A. Skerrett-Byrne[a,b,g,h], Shannon P. Smyth[a,b,i], Ilana R. Bernstein[a,b], Amanda L. Anderson[a,b], Simone J. Stanger[a,b], Ewan N. A. Simpson[a,b], Archana Tomar[g,h], Raffaele Teperino[g,h], Colin C. Conine[a,d,e,f], Geoffry N. De Iuliis[a,b], Shaun D. Roman[b,j], Elizabeth G. Bromfield[a,b,i], Matthew D. Dun[k,l], Andrew L. Eamens[m], and Brett Nixon[a,b,2]

Affiliations are included on p. 11.

Forecasted increases in the prevalence and severity of extreme weather events accompanying changes in climatic behavior pose potential risk to the reproductive capacity of humans and animals of ecological and agricultural significance. While several studies have revealed that heat stress induced by challenges such as testicular insulation can elicit a marked negative effect on the male reproductive system, and particularly the production of spermatozoa, less is known about the immediate impact on male reproductive function following subchronic whole-body exposure to elevated ambient temperature. To address this knowledge gap, we exposed unrestrained male mice to heat stress conditions that emulate a heat wave (daily cycle of 8 h at 35 °C followed by 16 h at 25 °C) for a period of 7 d. Neither the testes or epididymides of heat-exposed male mice exhibited evidence of gross histological change, and similarly, spermatozoa of exposed males retained their functionality and ability to support embryonic development. However, the embryos generated from heat-exposed spermatozoa experienced pronounced changes in gene expression linked to acceleration of early embryo development, aberrant blastocyst hatching, and increased fetal:placental weight ratio. Such changes were causally associated with an altered sperm small noncoding RNA (sncRNA) profile, such that these developmental phenotypes were recapitulated by microinjection of wild-type embryos sired by control spermatozoa with RNAs extracted from heat-exposed spermatozoa. Such data highlight that even relatively modest excursions in ambient temperature can affect male reproductive function and identify the sperm sncRNA profile as a particular point of vulnerability to this imposed environmental stress.

sperm | heat | embryo development | epididymis | small non-protein-coding RNA

Significance

The fidelity of sperm production underpins successful reproduction yet is highly vulnerable to various forms of environmental challenge, including heat stress. Despite this knowledge, we lack a complete understanding of the immediate impact on male reproduction of whole-body exposure to elevated ambient temperatures such as those encountered during a heatwave. By experimentally emulating heatwave conditions, we demonstrate that the spermatozoa of exposed mice accumulate changes in their small RNA profile that are causally linked to pronounced changes in embryonic gene expression, accelerated preimplantation development, aberrant blastocyst hatching, and increased fetal:placental weight ratio. Such data highlight that even a relatively modest elevation in ambient temperature can affect male reproductive function, demonstrating the acute sensitivity of sperm small RNAs to environmental stress.

[1]J.E.S. contributed equally to this work.

[2]To whom correspondence may be addressed. Email: brett.nixon@newcastle.edu.au.

Climate change models predict increases in global temperatures of between 1.1 to 6.4 °C by the end of this century (1). Irrespective of the magnitude of this change, there is incontrovertible evidence that our global environment is changing, such that each of the past four decades has been warmer than the previous one (1). Among the consequences of anthropogenic-driven climate change are more extreme weather events including longer and hotter summers and an increased prevalence and intensity of heat waves (1); defined as the number of successive days (typically 3 to 5 d), where maximum ambient conditions are above a specific threshold (2). While the climatic behavior of heat wave events varies from summer to summer (3), climate records allude to an increased frequency of such events since the 1990s (1). In regions such as southern Australia for instance, the average number of consecutive days of heat stress has increased from 2 d per heat stress event from 1960–1999, to 4 d from 2000–2008 (4). Moreover, recent heatwave events in western North America have been registered as among the most extreme events ever recorded globally (5). In anticipation of increasing trends of climate change and climate variability, there is a pressing need to develop a greater understanding of the impact such events will have on biological parameters in humans as well as animals of ecological and agricultural significance. Such an evidence-based approach will enable the development of efficacious mitigation strategies for improved animal welfare and productivity during periods of heat stress (1).

The impact of heat waves on animals is influenced by a variety of factors including the intensity and duration of the event. Moreover, susceptibility to prolonged heat wave events is exacerbated when night-time temperatures remain high, thereby limiting the dissipation of excess heat load (6, 7). Indeed, heat wave events are known to dysregulate the diurnal rhythm of body temperature thus impeding the capacity of an animal to

remain in thermal equilibrium with its environment (8). Once heat load increases beyond a physiological threshold, it initiates a cascade of behavioral, endocrine, and biochemical responses that function in parallel to minimize the adverse effects of heat stress on the whole-body (9–12). Of note, such responses frequently occur at the expense of reproductive fitness (13–15). In the context of male reproduction, heat stress has been linked to pronounced impacts on sperm production in the testis, a process that appears to be particularly susceptible to temperature flux (16). It follows that the male reproductive tract of most mammals features numerous complex anatomical structures and physiological mechanisms that combine to create a substantial temperature gradient between the body and testes (17, 18). Most notable of these specializations is the descent of the testicles into a scrotum, which permits optimal sperm production to proceed at temperatures that are generally some 2 °C to 4 °C below that of core body temperature. This temperature differential is regulated via the combined action of the tunica dartos and cremaster muscles, scrotal sweat glands, and most importantly, through the bidirectional flow of blood via the arteries and veins held within the spermatic cord; a system that results in countercurrent heat exchange to precool blood entering the testes (19, 20). However, this thermoregulation system is not infallible and can be overwhelmed in situations of prolonged heat load precipitating a rise in testicular temperature and attendant effects on both the quality and quantity of sperm produced. Indeed, several studies have linked even subtle elevations in scrotal temperature to negative impacts on the germinal epithelium, often reflected in elevated levels of apoptosis, DNA damage, and abnormalities of spermiogenesis within the developing germline (17, 21–28).

Notably, the majority of studies demonstrating the negative impact of heat stress on male reproductive function have utilized techniques, such as scrotal insulation, that directly impede the thermoregulatory capacity of the scrotum, but also obfuscate the highly coordinated whole-body behavioral and physiological mitigation responses (19, 26, 29–34). As a result of these isolated and somewhat "artificial" forms of heat challenge, there remain deficiencies in our knowledge regarding the true impact of heat stress on male reproductive function arising from whole-body exposure. Further, few studies have focused on the downstream consequences on semen characteristics resulting immediately after the exposure of a male to heat stress, when the exposed spermatozoa are residing within the epididymal lumen; a highly specialized region of the male excurrent duct system that is responsible for promoting the functional maturation of spermatozoa as well as the creation of a sperm storage reservoir (35, 36). This is despite mounting evidence that the epididymis not only displays sensitivity to a variety of environmental stressors, but that it can respond to such challenges via the production of stress signals that are subsequently relayed to the recipient population of luminal spermatozoa (35). Such stress signals frequently take the form of small noncoding RNAs (sncRNAs), which are conveyed to the epididymal lumen via extracellular vesicles, referred to as epididymosomes (37–39). This communication nexus between somatic cells of the epididymis and germ cells not only alters the epigenetic landscape of the maturing male gamete (40–44), but has increasingly been linked to the downstream dysregulation of early embryo development; changes that can, in turn, alter embryo developmental trajectory and even influence the lifelong health of offspring (40, 41, 45, 46). Whether such a causative pathway is initiated by whole-body heat stress such as that encountered during heat wave conditions remains an important and unresolved question. To address this knowledge gap, here, we utilized a tractable heat exposure regimen to assess the chain of cause and effect between elevated ambient temperature, changes in the sncRNA profile of epididymal spermatozoa, and altered embryo and fetal development.

Results

Heat Treatment Regimen. Adult male mice (8 wk old) were randomly assigned into heat-exposed or control groups and subjected to the treatment regimen (daily cycle of 8 h at 35 °C, followed by 16 h recovery at 25 °C; *SI Appendix*, Fig. S1*A*) for a 7-d period. The duration of heat exposure was selected to coincide with that encountered during a prolonged heat wave and with the transit period of spermatozoa through the epididymis. The ambient temperature of the heating apparatus was assessed using a temperature logger throughout the duration of the exposure period and revealed the attainment of a stable temperature environment (*SI Appendix*, Fig. S1*A*). Mice were monitored twice daily over the course of the treatment regimen with temperatures of the armpit, stomach, and scrotum assessed at the culmination of each heat cycle. While no change in temperature was observed at the armpit (*SI Appendix*, Fig. S1*B*), both the stomach (2.4% increase, $P \leq 0.05$, *SI Appendix*, Fig. S1*C*) and scrotum/testes (9.4% decrease, $P \leq 0.05$, *SI Appendix*, Fig. S1*D*) temperatures were significantly altered. In accounting for the latter observation, it was noted that the testes appeared more descended into the scrotal cavity in heat-exposed animals compared to that of their control counterparts. After all animals were killed on the morning of day 8, it was revealed that the imposed heat stress regimen did not influence overall mouse weight (*SI Appendix*, Fig. S1*E*), nor the weight of any tissues examined (*SI Appendix*, Fig. S1 *F–I*).

Epididymal Physiology Is Not Overtly Affected by Subchronic Heat Stress. As the focus for this study, the epididymides of heat-exposed animals did not present with any overt changes in gross morphology (*SI Appendix*, Fig. S2*A*). Accordingly, we also failed to detect any signatures of heat-induced damage to the epithelial cells that line the epididymal lumen as assessed by probing for the formation of oxidative DNA adducts (*SI Appendix*, Figs. S2*B* and S3*A*), the expression of single-stranded DNA lesions (*SI Appendix*, Figs. S2*C* and S3*B*) and the induction of apoptosis (*SI Appendix*, Figs. S2*D* and S3*C*). Combined, these assays detected only modest numbers of individual epididymal epithelial cells displaying positive staining for 8-hydroxy-2'-deoxyguanosine (8-OHdG), TUNEL, or caspase-3 probes. Moreover, the proportion of labeled cells was not elevated by the imposed heat stress regimen (*SI Appendix*, Figs. S2 *B–D* and S3 *A–C*). Similar to the response of the epididymis, heat exposure also failed to elicit any pronounced changes in the gross morphology of the testes of exposed animals (*SI Appendix*, Fig. S3*D*). The imposed exposure regimen did, however, influence the fidelity of testicular germ cell development as evidenced by a modest increase in DNA damage (i.e., 8-OHdG labeling; *SI Appendix*, Fig. S3*E*) and an attendant elevation, albeit subtle, in the expression of apoptosis markers (i.e., TUNEL, caspase 3; *SI Appendix*, Fig. S3 *F* and *G*) among the germ cells of heat challenged males. Notwithstanding these effects, abundant spermatozoa were detected within the lumen of all epididymal segments of exposed males (*SI Appendix*, Fig. S2*A*).

Mature Sperm Function Is Not Compromised by Subchronic Heat Stress. Consistent with epididymal tissue appearing largely unaffected by subchronic heat stress, the mature cauda epididymal spermatozoa of heat-treated animals (i.e., populations of spermatozoa that would have solely resided in the epididymis during heat exposure) also revealed no compromise in total sperm count (*SI Appendix*, Fig. S4*A*), sperm viability
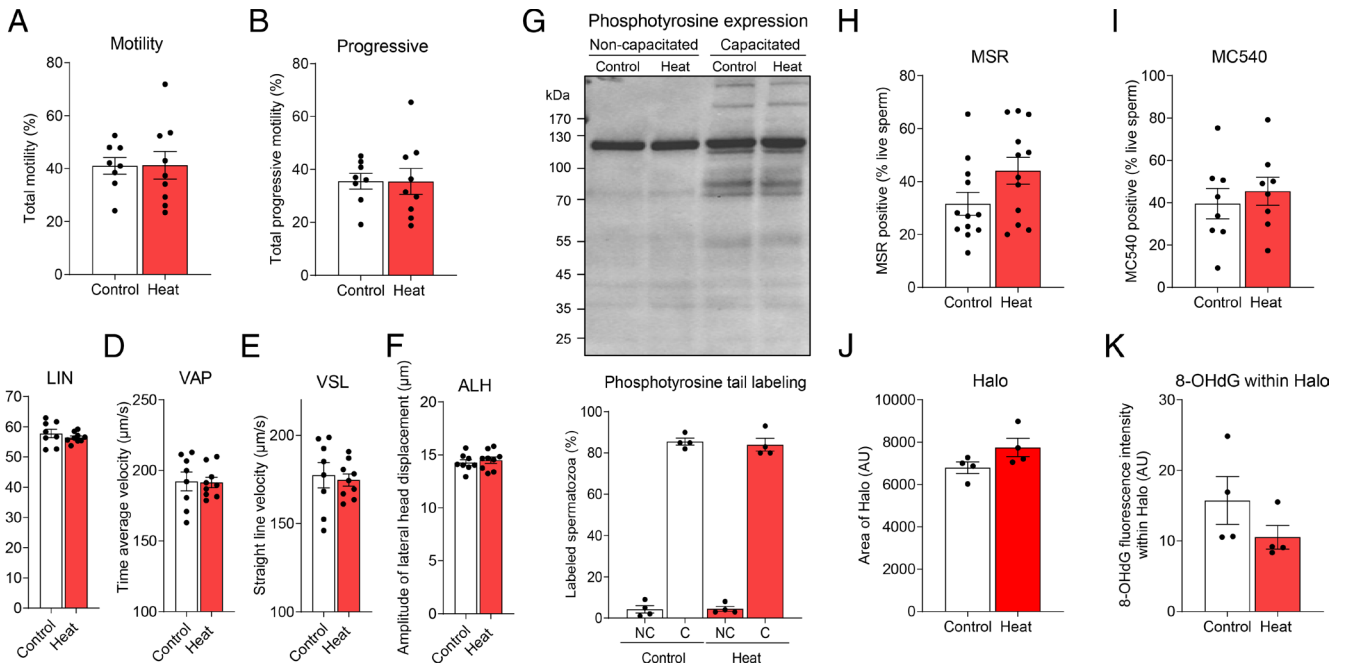
Fig. 1. Effect of paternal heat stress on the quality of mouse spermatozoa. At necropsy, cauda epididymal spermatozoa were isolated from heat-treated or control mice and prepared for assessment of (A–F) motility parameters. Several sperm motility and velocity parameters were objectively assessed via CASA including (A) total motility, (B) progressive motility, (C) linearity (LIN, %), (D) average path velocity (VAP, μm/s), (E) straight line velocity (VSL, μm/s), and (F) amplitude of lateral head displacement (ALH, μm). (G) Spermatozoa were also induced to undergo in vitro capacitation before assessment of tyrosine phosphorylation status via immunoblotting of cell lysates and immunostaining of fixed cells with anti-phosphotyrosine antibodies. Additional measures of sperm quality including (H) MSR, (I) sperm membrane fluidity (MC540), (J) area of Halo, and (K) intensity of 8-OHdG labeling within the sperm Halo were also recorded. Data are presented as mean ± SEM having been calculated based on the assessment of spermatozoa from n = 4 to 12 mice/group for each assay; circle symbols depict values obtained from populations of spermatozoa from individual mice. Differences between groups were assessed by unpaired Student's t test for normally distributed data or unpaired Mann–Whitney test for data not normally distributed.

(*SI Appendix*, Fig. S4B), or their motility characteristics as assessed using computer-assisted sperm analyses (CASA; Fig. 1 A–F and *SI Appendix*, Fig. S5). Similarly, populations of heat-exposed spermatozoa retained the ability to undergo capacitation (Fig. 1G) and did not present with any characteristic signatures indicative that they may harbor an elevated burden of oxidative stress: as assessed using probes to detect mitochondrial ROS generation (MSR) (Fig. 1H), membrane integrity (Fig. 1I), and DNA integrity (Fig. 1 J and K).

It follows that the spermatozoa of heat-exposed sires retained the ability to fertilize oocytes in both an in vitro (Fig. 2A) and in vivo (Fig. 3A) setting. In terms of the former, the in vitro fertilization (IVF) rate (Fig. 2A) and subsequent developmental potential (as measured by the number of 2-cell embryos that developed to a blastocyst; Fig. 2B) proved equivalent for embryos produced with spermatozoa from both heat-exposed and control sires. However, in assessing embryo progression through landmark developmental stages (Fig. 2 C–F), we noted that cultured embryos generated with heat-exposed spermatozoa were advanced beyond that of the rate of development of their control counterparts (Fig. 2 E and F). This difference in developmental trajectory was first detected at 72 h postfertilization where we noted a decrease in the proportion of embryos at the morula stage ($P \le 0.05$), and proportional increase in embryos that had developed to the early blastocyst stage ($P \le 0.05$) (Fig. 2E). Further, this trend was observed to continue through to the proportion of hatching/hatched blastocysts at 96 h (Fig. 2F). An apparent consequence of this accelerated embryo development was aberrant blastocyst hatching from within the encircling zonae pellucidae (Fig. 2 G–K). In this context, almost half of all embryos generated with heat-exposed spermatozoa that developed to the blastocyst stage displayed multiple, randomly distributed hatching sites, an anomaly that was detected in <10% of embryos sired by spermatozoa from

control males (Fig. 2G, $P \le 0.01$). However, investigation of embryos with anomalous hatching sites revealed this phenotype was not associated with an overt loss of cytoskeletal integrity (Fig. 2I) or increased DNA damage (Fig. 2 J and K) among blastomeres emerging from either a single or multiple hatching foci.

Increased Fetal Weight and Changes in Placental Architecture Are Detected Among Fetuses Sired by Heat-Exposed Males. In consideration of the blastocyst hatching anomalies witnessed in embryos generated by the spermatozoa of heat-exposed males, we elected to examine whether this exposure regimen compromised implantation or pregnancy outcomes. Thus, heat-exposed males and their control counterparts were mated with unexposed virgin females, with no difference in average time to mating between control (2.8 d) and heat-exposed males (2.9 d). Prior to term on day 17.5 postcoitum (pc), females were killed, and late gestation pregnancy parameters were assessed. This analysis revealed no difference in the number of females with at least one viable fetus (Fig. 3A), the number of implantation sites (Fig. 3B), the number of viable implantation sites (Fig. 3C), percentage of fetal resorptions (Fig. 3D), or sex distribution among fetuses (Fig. 3 E and F). Notwithstanding these outcomes, paternal heat exposure heralded a trend towards increased fetal weight (Fig. 3G, $P = 0.056$). Without a commensurate increase in placental weight (Fig. 3H), this phenomenon led to a significant increase in fetal:placental weight ratio (a measure of placental efficiency) in offspring sired by heat-exposed males compared to control males (Fig. 3I, $P \le 0.05$). The sex of the offspring did not overtly influence these phenotypes (*SI Appendix*, Fig. S6 A–F). Notably, despite equivalent placental weights, we did record a trend towards increased overall surface area of the placenta ($P = 0.09$, Fig. 3 J, N, and O) in embryos sired by heat-exposed males. Such changes were primarily attributed to a significant increase in the area of the labyrinth zone (Fig. 3K,
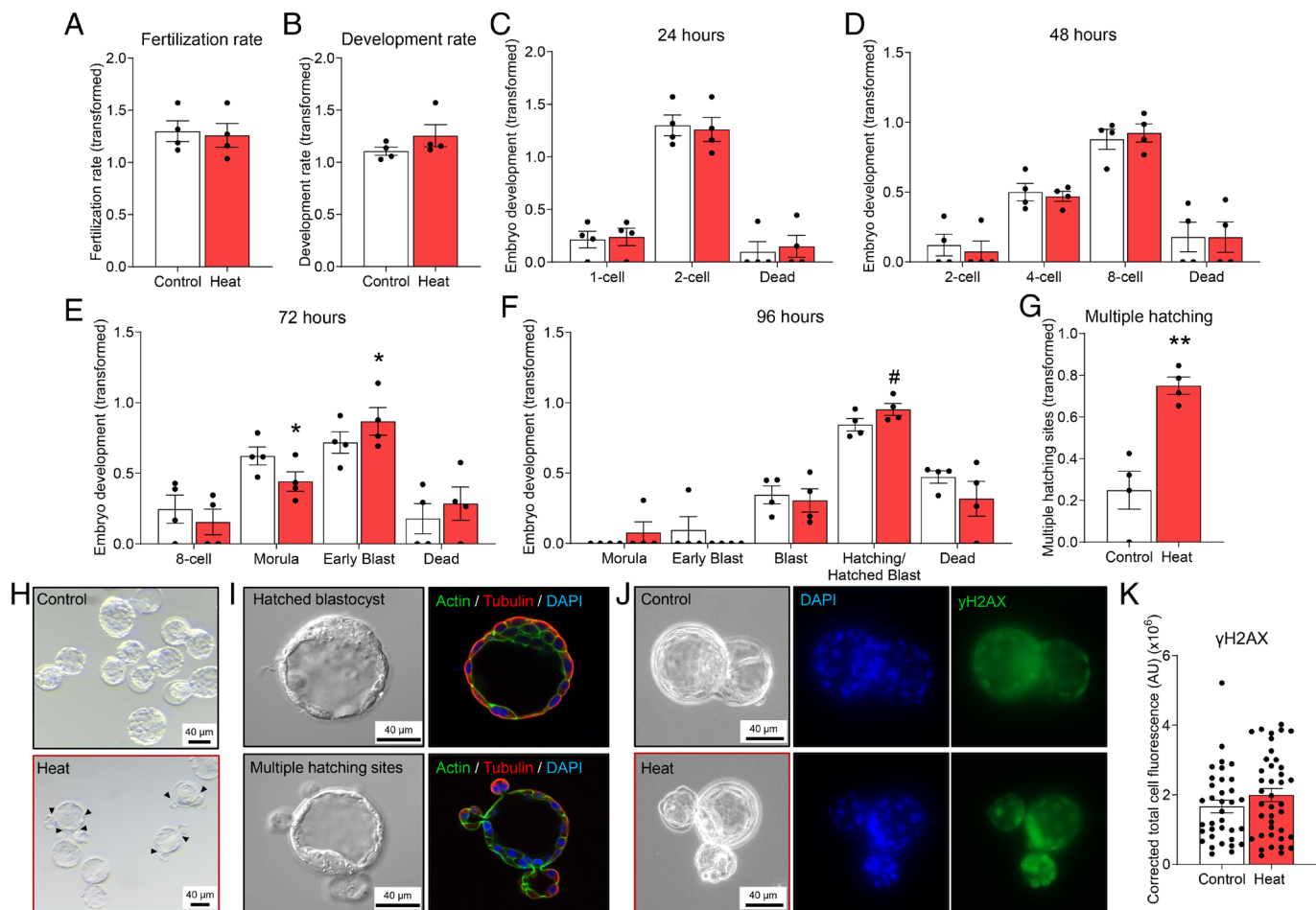
Fig. 2. Impact of paternal heat stress on IVF and embryo development. Cauda epididymal spermatozoa from control and heat-exposed mice were isolated and added into droplets containing oocytes from untreated females to permit IVF. Note that all data are presented as arcsine transformed values and each circle symbol represents an individual IVF experiment (i.e., replicate) featuring the spermatozoa from one male and oocytes from six female mice. (*A*) The number of fertilized oocytes after 4 h of gamete coincubation was recorded, and data are presented as the transformed total 2-cell embryos at 24 h. (*B*) Zygotes were cultured for 96 h during which development was tracked. The development rate for each group is represented as transformed data based on the proportion of 2-cell embryos that developed to blastocyst. The developmental stage of embryos sired from control and heat-exposed spermatozoa at (*C*) 24, (*D*) 48, (*E*) 72, and (*F*) 96 h is depicted. (*G*) Following 96 h of culture, the number of embryos displaying multiple hatching sites was recorded and presented as transformed data based on the percentage of hatching blastocysts. (*H*) Representative phase images of embryos cultured for 96 h are presented to illustrate the phenomenon of embryos with multiple hatching sites (black arrowheads). (*I*) Blastocysts were stained for polymeric actin (phalloidin-fluorescein isothiocyanate; green) and alpha tubulin (red) prior to counterstaining with the nuclear marker, DAPI (blue). Representative phase and merged images captured by confocal microscopy are presented. (*J*) Alternatively, blastocysts were dual stained for γH2AX (green), a molecular marker of DNA damage (specifically, DNA double-strand breaks), and DAPI (blue). (*K*) Quantitation of γH2AX foci was performed using corrected total cell fluorescence (CTCF) protocols and graphical data are presented as mean ± SEM wherein circle symbols depict the CTCF values recorded in individual embryos (n = 36 or n = 40 embryos fertilized with the spermatozoa of control or heat-treated males, respectively). Embryo development data were arcsine transformed prior to statistical analysis. Differences between groups were assessed by (*A–G*) paired Student's *t* test for normally distributed data, or paired Wilcoxon matched-pairs signed-rank test for data not normally distributed, or (*K*) unpaired Mann–Whitney test for data not normally distributed. * indicates $P \leq 0.05$, # indicates $P \leq 0.1$. (*H–J*) (Scale bars, 40 μm.).

$P \leq 0.05$) and accompanying trends toward increased junctional zone (Fig. 3*L*, $P = 0.09$) and decidual zone area (Fig. 3*M*, $P = 0.07$).

The Small RNA Profile of Epididymal Spermatozoa Is Altered by Subchronic Heat Exposure. In the absence of an overt loss of DNA integrity in heat-exposed epididymal spermatozoa (Fig. 1 *J* and *K*) that could account for altered embryo development (Fig. 2 *E* and *F*), we elected to focus on alternative stress signals that may be communicated to the oocyte and subsequent fetus via the spermatozoa of heat-exposed males. Based on previous work emphasizing the propensity of diverse paternal stressors to manifest in an altered sncRNA landscape among the spermatozoa of stressed fathers (38), we prioritized the profiling of variations in these epigenetic signals. Specifically, mature spermatozoa isolated from the cauda epididymis of experimental cohorts of mice were prepared for sequencing of the sncRNA fraction, that being: RNA molecules 18 to 40 nucleotides in length. This strategy identified a profile of sncRNA dominated by transfer RNA

fragments (tRFs), representing 45.6 and 32.8% of total genome mapped reads within the spermatozoa of control and heat-exposed mice, respectively (Fig. 4*A* and *SI Appendix*, Tables S1–S4). The overall sncRNA size distribution profile was largely comparable between both samples, barring a reduction in sncRNAs of 31 to 33 nucleotides in length, particularly those sncRNAs belonging to the tRF class, in sperm from heat-exposed mice (Fig. 4*B*). Accordingly, assessment of differential abundance of each sncRNA class revealed that heat exposure altered the accumulation of 7.1% of detected tRFs, with the majority of these (5.9%) displaying decreased abundance in sperm from heat-exposed mice (Fig. 4*C* and *SI Appendix*, Table S2). Heat exposure–induced alteration of the sncRNA landscape of cauda epididymal sperm was also evident for the other sncRNA classes detected by small RNA-seq. Namely, proportional increases were detected for the PIWI-interacting RNA (piRNAs) and ribosomal RNA fragment class of sncRNA, and further, decreased abundance was determined for the microRNA (miRNA) sncRNA class. (Fig. 4*A*). These changes
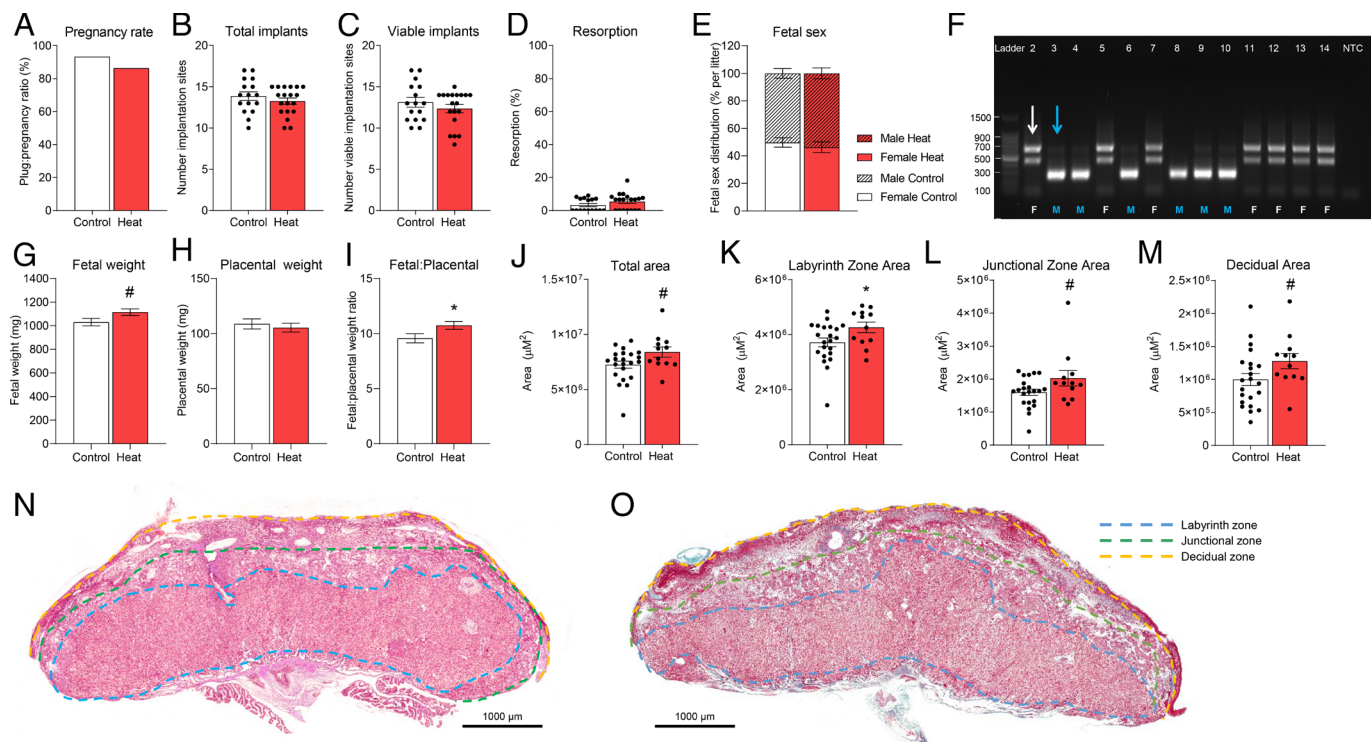
Fig. 3. Effect of paternal heat stress on pregnancy outcomes. At the completion of their treatment regimen, heat-exposed and control male mice (n = 14 per treatment) were mated with untreated females (n = 2 per breeding pair). Thereafter, females were killed at 17.5 d postcoitus, and the following parameters were assessed: (*A*) Plug:pregnancy ratio (defined as the number of mated females with at least one viable implantation site), (*B*) total number of implantation sites per pregnant mouse, (*C*) total number of viable implantation sites per pregnant mouse, and (*D*) the proportion of implantation sites per pregnant female undergoing resorption. (*E*) Genomic DNA from fetal tail clippings was used to determine fetal sex. (*F*) Representative gel image of *Sly/Xlr* gene products amplified by PCR. This approach yields 685-bp, 660-bp, and 480-bp products for female gDNA (i.e., white arrow; F) or alternatively, a 280-bp amplicon and often faint "X chromosome" bands for male gDNA (i.e., blue arrow; M). Lane 1 contains a 100 bp DNA ladder; lanes 2 to 14 contain fetal gDNA; lane 15 contains a no template control (NTC) sample. (*G*) Fetal weight, (*H*) placental weight, and (*I*) fetal:placental weight ratio (surrogate marker for placental efficiency). Assessment of the placenta was performed on histological sections stained with Masson's trichrome, and the (*J*) total area, as well as the area of the (*K*) labyrinth, (*L*) junctional, and (*M*) decidual zones, was recorded. Representative images of fetal placentae from pups sired by either (*N*) control or (*O*) heat-exposed males are depicted, with dashed lines demarcating the boundaries of the different zones assessed in this study. (Scale bars, 1,000 μm.). Graphical data are presented as (*B–D* and *J–M*) mean ± SEM values with circle symbols depicting values from individual mice or (*G–I*) estimated marginal mean ± SEM. The effect of heat stress was assessed from n = 16 to 19 litters by (*A* and *E*) chi-square analysis, (*B–E* and *J–M*) unpaired Student's *t* test for normally distributed data or unpaired Mann–Whitney test for data not normally distributed, and (*G–I*) Generalized Linear Mixed Model and post hoc least significant difference test, with the subject as father (mother nested) and viable pups as a covariate. * indicates P ≤ 0.05; # indicates P ≤ 0.1.

corresponded to 7.1% of the detected piRNAs, and 1.8% of the detected miRNAs exhibiting significantly altered abundance in heat-exposed, compared to control spermatozoa (Fig. 4*C* and *SI Appendix*, Tables S1–S4).

Embryos Generated with the Spermatozoa of Heat-Exposed Males Display Altered Profiles of Preimplantation Gene Expression. To begin to explore downstream implications of changes in the sncRNA landscape of heat-exposed spermatozoa, transcriptomic profiling was conducted on 4-cell embryos (timed to follow the robust wave of zygotic genome activation that occurs in 2-cell stage mouse embryos) and morula stage embryos generated by IVF. This strategy revealed a total of 15,887 detectable gene transcripts, approximately 9.6% of which proved responsive to paternal heat exposure in 4-cell embryos (Fig. 5*A* and *SI Appendix*, Table S5). In this context, differentially expressed genes (DEGs) (*P*-value ≤ 0.05 and fold change ±1.5), comprised 406 (2.6%) down-regulated and 1,117 (7.0%) up-regulated transcripts, via comparison of embryos generated from heat-exposed and control populations of spermatozoa (Fig. 5*A*). Curiously, despite the potential repercussions of such changes in terms of the developmental trajectory of embryos, an equivalent transcriptomic analysis performed on more advanced morula stage embryos revealed far more subtle dysregulation of gene expression. Indeed, determination of DEGs in morula embryos generated by heat-exposed spermatozoa revealed

339 (2.1%) down-regulated and 91 (0.6%) up-regulated genes, via comparison with embryos sired by control spermatozoa (Fig. 5*D* and *SI Appendix*, Table S9). In comparing the DEGs in 4-cell and morula embryos fertilized by heat-exposed compared to control spermatozoa we identified 13 up-regulated and 25 down-regulated genes equally affected at both developmental stages (*SI Appendix*, Tables S5 and S9; highlighted in purple).

Focusing on the gene expression differences at the 4-cell embryo stage, Ingenuity Pathway Analysis (IPA) software revealed a number of dysregulated canonical pathways and predicted upstream regulators of DEGs linked to early embryonic development, including the putative inhibition of several endogenous miRNAs that may influence the detected gene expression changes (*SI Appendix*, Fig. S7 *A–D* and Tables S6–S8). Consistent with the phenotypes of accelerated embryo development and increased fetus weight documented above (Figs. 2 *E* and *F* and 3*G*), 4-cell embryos sired by the spermatozoa of heat-exposed males exhibited a DEG signature associated with the activation of signaling networks promoting body size, cell survival, and cell viability (Fig. 5*B* and *SI Appendix*, Table S8). Conversely, embryos fertilized by heat-exposed sperm also featured an inhibition of cellular functions linked to organismal death and growth failure (Fig. 5*C*). Comparatively, the panel of DEGs in morula embryos originating from heat-exposed spermatozoa mapped to a spectrum of canonical pathways, upstream regulators, and cellular functions
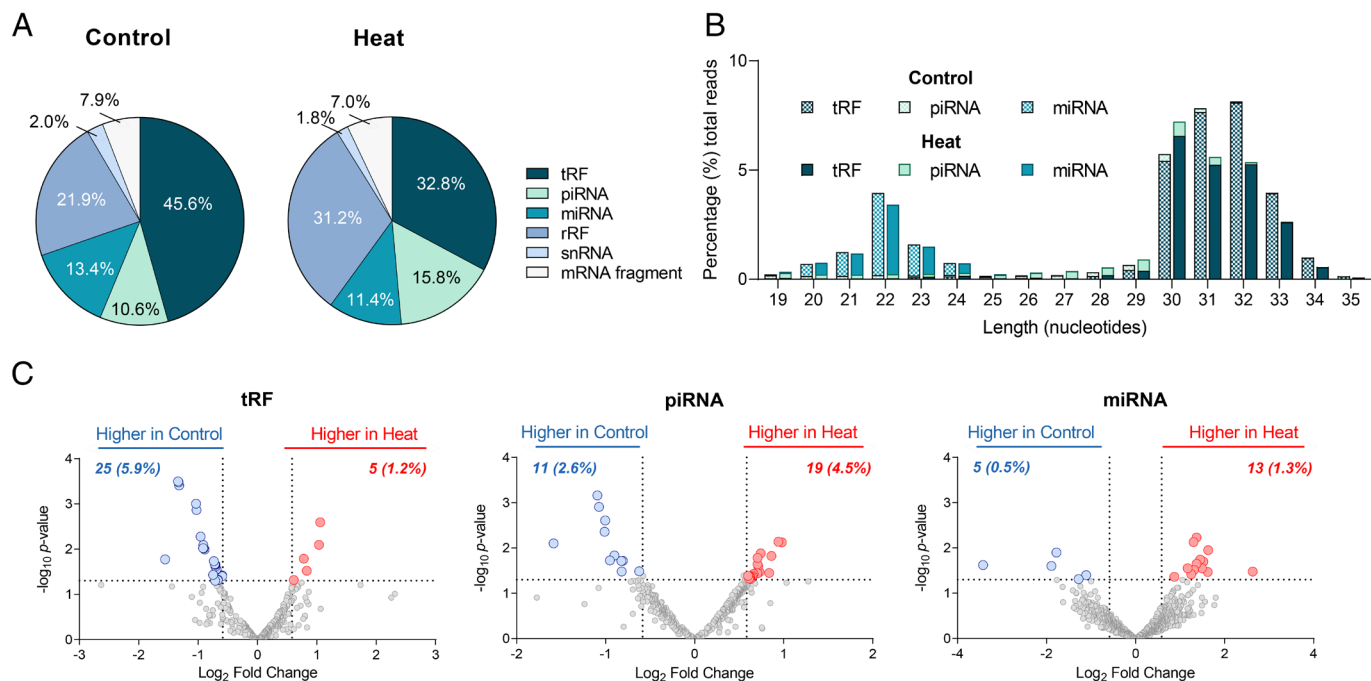
Fig. 4. The influence of heat stress on the sncRNA payload of cauda epididymal spermatozoa. At the cessation of heat exposure, spermatozoa were isolated from the cauda epididymides of control and heat-treated mice and prepared for sncRNA isolation and sequencing (n = 3). (*A*) Proportional contribution of each sncRNA subclass to the global sncRNA payload of control and heat-exposed spermatozoa. (*B*) Size distribution of tRFs, piRNA, and miRNA mapping sncRNA transcripts. Data represent average of three replicates for each treatment group. (*C*) Volcano plots depicting differentially accumulated sperm sncRNAs from heat-exposed compared to control males. Blue and red circle symbols denote individual sncRNAs that were either significantly reduced or increased in abundance in heat-exposed compared to control spermatozoa, respectively. Graphical data are presented as mean values of three biological replicates. The effect of heat stress was assessed by (*B*) an unpaired *t* test or (*C*) DESeq2, represented by volcano plots of tRF, piRNA, and miRNA expression values with a significance threshold of fold change ± 1.5 and *P*-value ≤ 0.05.

associated with the compromise of cellular metabolism (e.g., activation of disorders of glucose metabolism) and cell viability (e.g., activation of cell death and inhibition of cell viability) (Fig. 5 *E* and *F* and *SI Appendix,* Fig. S7 *E–H* and Tables S10–S12).

Accompanying other forms of epigenetic regulation, sperm miRNAs delivered to the oocyte at the time of fertilization are known to influence early embryonic development (47). Accordingly, we next examined the potential influence of sperm miRNA changes elicited in response to heat exposure on the early embryo transcriptome. For this purpose, the MicroRNA Target Prediction Database database (48) was interrogated to generate a list of predicted gene targets for miRNAs altered in heat-exposed spermatozoa. The generated miRNA target gene list was then filtered to identify the predicted target genes that match 4-cell DEGs, as the earlier developmental stage. As part of this analysis, we placed an additional and specific focus on identifying miRNA/mRNA target genes determined to have reciprocal expression trends. More specifically, we focused our attention on expression modules where target gene expression was repressed in 4-cell embryos while the abundance of their corresponding miRNAs was increased in heat-exposed spermatozoa, and vice versa (i.e., increased target gene expression, and decreased abundance of the targeting miRNA). This strategy identified a subset of 278 genes in 4-cell embryos putatively targeted by heat-responsive sperm miRNAs (*SI Appendix,* Table S13). IPA assessment mapped this cohort of DEGs to several functional categories, including the identification of 27 genes linked to activation of "size of body" (Z-score = 2.36) in embryos sired by heat-exposed spermatozoa (Fig. 6). Notably, each of the heat-responsive sperm miRNAs displayed reciprocal abundance profiles to that of their targeted embryonic genes, such that *miR-6931, miR-7240, miR-376c, miR-219a-2,* and *miR-741* were each characterized by

reduced abundance in the spermatozoa of heat-exposed males yet a subset of their predicted target genes were detected at higher expression levels in the embryos sired by this population of spermatozoa (Fig. 6, left-hand side). Conversely, the abundance of *miR-423, miR-7217, miR-7242, miR-7234, miR-380, miR-92b,* and *miR-7214* was elevated in heat-exposed cauda spermatozoa, and the expression level of their respective predicted target gene(s) was reduced in 4-cell embryos fertilized by heat-exposed spermatozoa (Fig. 6, right hand side, *SI Appendix,* Table S13). Together, these analyses identify a cohort of early embryonic genes with profiles of altered expression potentially influenced by miRNA changes in spermatozoa exposed to short-term heat stress.

To further explore the prospect that heat-responsive miRNAs (and potentially other forms of sperm RNAs) may be exerting regulatory control over early embryonic gene networks, RNA harvested from the spermatozoa of heat-exposed males was microinjected into wild-type embryos sired by the spermatozoa of control males prior to tracking embryo development over 96 h (Fig. 7*A*). This strategy largely recapitulated the phenotype of accelerated early embryo development originally witnessed in embryos sired by heat-exposed spermatozoa. Thus, despite no difference in development rate (Fig. 7*B*) or developmental potential up until 48 h postfertilization (Fig. 7*C*), by 72 h postfertilization, we witnessed proportionally more morula embryos arising in those embryos supplemented with RNAs from heat-treated spermatozoa (*P* ≤ 0.05) (Fig. 7*D*). This trend of accelerated embryo development continued to the final time point assessed (i.e., 96 h postfertilization) at which time we recorded a notable increase in early and late blastocysts (*P* = 0.085) (Fig. 7*E*). Taken together, these data implicate heat-sensitive sperm RNAs as causative agents underpinning phenotypic changes in embryo development.
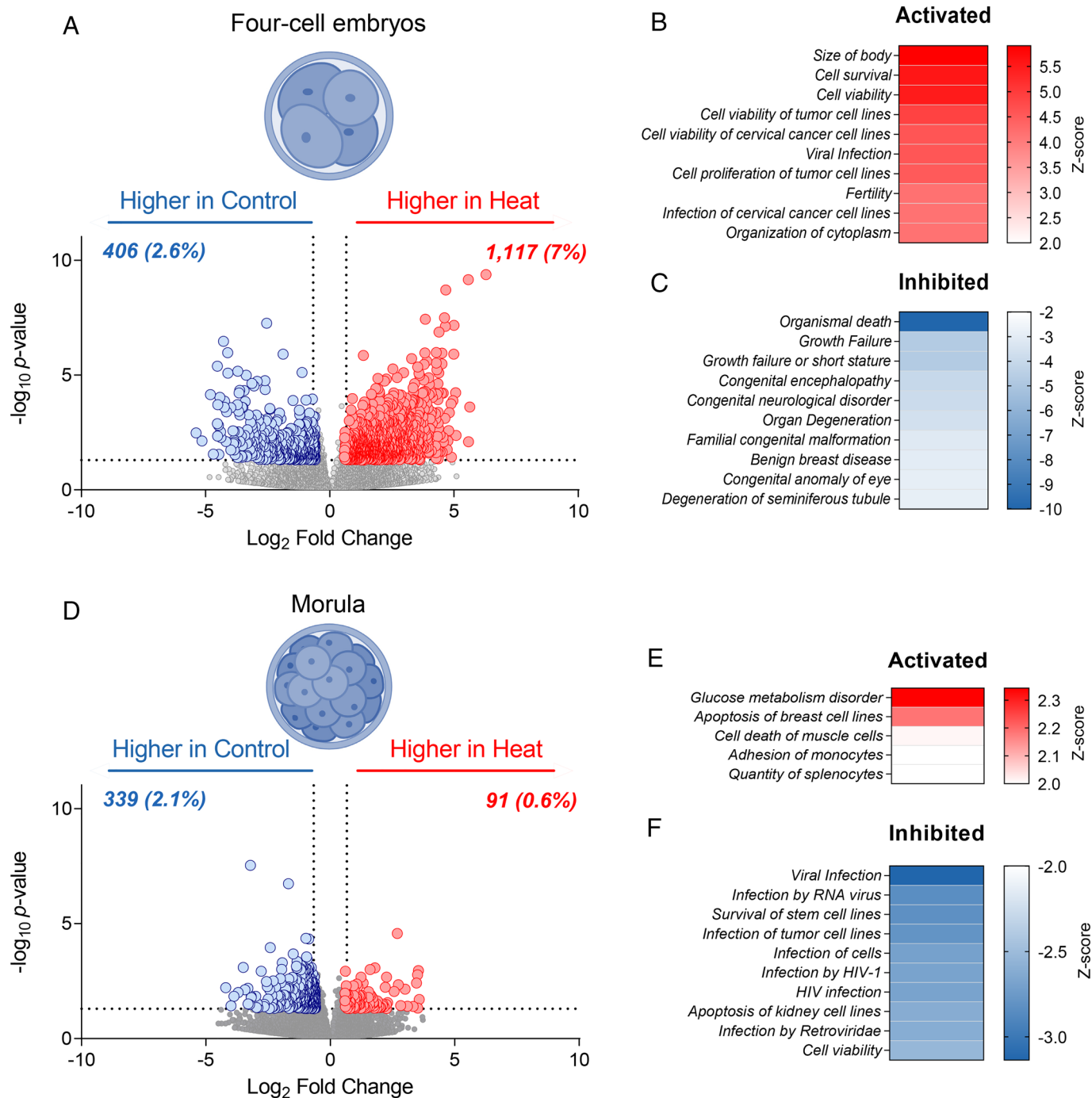
Fig. 5. The legacy of paternal heat stress on the preimplantation embryo transcriptome. Following IVF, embryos were cultured for either (*A–C*) 46 h (i.e., 4-cell embryos) or (*D–F*) 72 h (i.e., morula embryos) before being prepared for single embryo mRNA-Seq (n = 16 to 22 single embryos per group). (*A* and *D*) Volcano plots depicting fold change (x-axis, log2) and *P*-value (y-axis, −log10) of identified mRNA transcripts in 4-cell and morula stage embryos generated with spermatozoa from heat-exposed compared to control sires. Blue and red circle symbols indicate individual genes deemed to be significantly down- and up-regulated (*P*-value ≤0.05 and fold change ±1.5) in embryos sired by the spermatozoa of heat-exposed males, respectively. (*B, C, E,* and *F*) Highest ranked disease and functions identified by Ingenuity Pathway Analysis (IPA) software as being either (*B* and *E*) activated or (*C* and *F*) inhibited in embryos fertilized with the spermatozoa of heat-exposed compared to control males.

Discussion

The prospect of anthropogenically driven climate change and attendant forecasts of longer and hotter summers and more severe and frequent heat wave events (49) highlight a pressing need for improvements in our fundamental understanding of the patho-physiological impacts of heat stress on humans and animals of economic and ecological importance. In this context, there is mounting evidence that hot climatic conditions may already be having a deleterious impact on male reproductive capacity brought about by subversion of testicular thermoregulation and associated declines in semen quality (50). Building on these observations, the primary finding of this study was that whole-body exposure of mice to elevated ambient temperature designed to emulate a relatively modest heat wave event can elicit a rapid and marked effect on the sperm sncRNA landscape. Consistent with the demonstration that these epigenetic changes were not accompa-nied by a loss of DNA integrity or overt changes in the functional
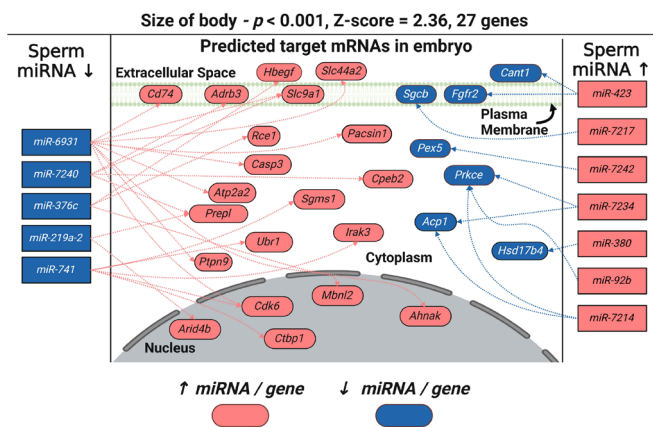
Fig. 6. Representative network analysis linking heat-sensitive sperm miRNAs to dysregulation of embryo gene expression. The MicroRNA Target Prediction Database software was used to identify the predicted gene targets of miRNAs that were differentially accumulated in the spermatozoa of heat-exposed males and that were themselves dysregulated in the 4-cell embryos generated from this population of spermatozoa. These data were interrogated using IPA to determine embryonic cellular pathways that may be susceptible to dysregulation by heat-associated changes in the sperm miRNA landscape. Among the dysregulated pathways identified by this strategy, "size of body" is presented to illustrate the reciprocal relationship that exists between the expression profile of heat-sensitive sperm miRNAs and that of their predicted target genes in 4-cell embryos. Specifically, red = up-regulated miRNAs/genes, blue = down-regulated miRNAs/genes, and connecting lines indicate the interaction network between sperm miRNAs and the embryonic genes they are predicted to regulate. The network schematic was initially generated by IPA before being redrawn using BioRender software (BioRender).

profile of heat-exposed epididymal spermatozoa, these cells retained the ability to sire embryos in both an in vitro and in vivo setting. The altered epigenetic profile of heat-exposed spermatozoa was, however, linked with an acceleration of early embryo development and an aberrant program of embryonic gene expression, etiologies that manifest in the dysregulation of blastocyst hatching, altered placental architecture, and increased fetal:placental weight ratio.

Heat stress ranks highly among the growing concerns inextricably linked with climate change, a global phenomenon that has already begun to herald an increased frequency of extreme weather events (49). As might be expected, however, the deleterious effects of heat stress vary in accordance with the timing, nature, and the severity of heat exposure. Indeed, core body temperature is not only influenced by the amount of heat accumulated but also the rate of heat load dissipation between the animal and its immediate environment. It follows that heat stress is accentuated by dysregulation of the diurnal rhythm of body temperature dissipation brought about when elevated daytime temperatures are accompanied by increased night-time temperatures, such as those imposed in the current study to emulate the impact of heat wave conditions. In species such as cattle for instance, it has been reported that peaks in body temperature lag ambient conditions by 8 to 10 h (7, 8). By contrast, during heat wave events (32 ± 7 °C), the lag between body temperature and ambient temperature decreases to 3 to 5 h (7, 8). This suggests that sustained hot conditions impede the capacity of an animal to remain in thermal equilibrium with its environment. Accordingly, as evidence of the elevation of heat load generated under the conditions imposed in this study, we observed a significant increase in body temperature measured on the stomach of exposed animals. Perhaps surprisingly, this was accompanied by a reciprocal decrease in testicular temperature, presumably brought about by the activation of physiological mechanisms, specifically, further descent of the testes into the scrotal cavity. Hence, the consequent impacts on epididymal

spermatozoa could arise from systemic signals in response to whole-body heat exposure or the responsive decrease in scrotal temperatures. Regardless, the observed physiological response likely occurs to minimize the impact on the male reproductive tract under conditions that exceeded the animals thermoneutral zone (51). The inability of this physiological thermoregulation response to effectively mitigate the adverse effects of prolonged elevated temperatures was highlighted at the molecular level by the observed increase to the burden of oxidative DNA damage in developing germ cells present within the testes of heat-exposed animals. These results are consistent with previous studies reporting that even modest heat load adversely affects spermatogenesis (16). However, this response proved sublethal and was not recapitulated among equivalent populations of epididymal spermatozoa, a finding that resonates with previous work illustrating a latency period of ~1 to 2 wk post heat insult before ejaculates first feature abnormal spermatozoa (33). This lag likely reflects the passage of time between release of spermatozoa from the testes and their subsequent transit through the epididymis (35). Although this implies that sperm cells held within the luminal environment of the epididymis are afforded additional protection from heat insult, presumably due to the presence of an exceptionally rich array of antioxidants within the lumen and the highly condensed nature of the paternal genome within the sperm head (52, 53), this does not preclude the possibility that they harbor alternative stress signals such as sncRNAs which until now, have not formed a primary focus of previous work in this field (37).

Over the past decade, the epididymis has drawn renewed interest not only because of its contributions to promoting the functional maturation of spermatozoa but also in recognition that it plays a fundamental role in establishing the epigenetic program carried by the fertilizing spermatozoon (35, 37, 38). Indeed, extending beyond its well-studied roles in remodeling of the sperm membrane and protein architecture compatible with navigation of the female reproductive tract and subsequent productive interactions with the ovum (54), it has become apparent that the epididymis actively contributes to the dynamic transformation of the sperm sncRNA landscape (40, 41, 43, 44). Such posttesticular changes to the sperm epigenome have, in turn, been linked to the downstream regulation of preimplantation embryo development, with experimental data supporting an essential, as opposed to ancillary, role in supporting early embryonic gene expression programs (40, 41, 43, 44). Notably, beyond the transmission of information pertinent to the physiological maturation of spermatozoa, the epididymis has also been implicated as a key conduit for communication of stress signals arising in response to a variety of paternal experiences (55). In this context, a substantial body of experimental data indicates that environmental stressors as diverse as isolated traumatic events through to chronic nutritional perturbations can converge to alter the sncRNA cargo carried by the male germline with implications for intergenerational inheritance of altered offspring phenotypic traits (45, 56). In a recent study, we have implicated the proximal segments of the epididymis in the propagation of such responses (39). Thus, we have shown that the somatic epithelial cell lining of the caput epididymis is sensitive to paternal exposures and responds to these challenges by recasting the proteomic landscape leading to an upregulation of a subset of transcription factors responsible for regulating, among other targets, the expression of *MIR* genes. Such changes culminate in altered production of a specific subset of miRNAs, which are thereafter relayed to the population of recipient spermatozoa residing in the epididymal lumen at the time of exposure. This mechanistic chain of cause and effect resonates with the findings of this study in which we showed that changes in the epididymal
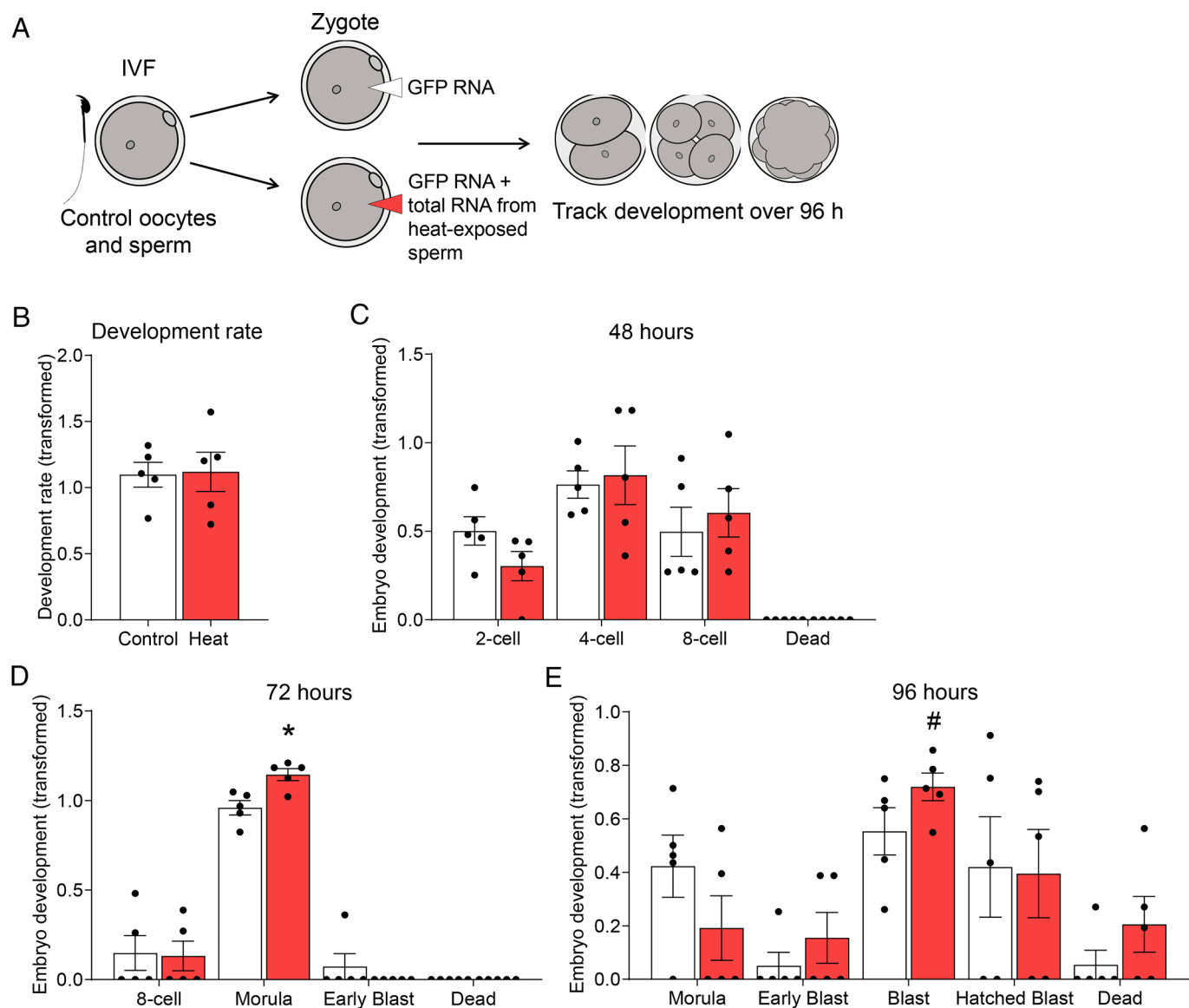
Fig. 7. The impact of heat-exposed sperm RNA on embryo development. (*A*) Zygotes generated by conventional IVF were microinjected with total RNA isolated from the spermatozoa of either control male mice or those subjected to heat stress. Note that all data are presented as arcsine transformed values and each circle symbol represents an individual IVF/microinjection experiment (i.e., replicate) in which naïve control mice were used as initial oocyte (3 to 4 females) and sperm (1 male) donors. (*B*) Development of embryos at 24 h postfertilization that were injected with control or heat-exposed sperm RNA. Embryos were cultured until 96 h, and development was recorded at intervals of (*C*) 48 h, (*D*) 72 h, and (*E*) 96 h. Graphical data depict the arcsine transformed value calculated from the percentage of 2-cell embryos at each developmental milestone and are presented as mean ± SEM. Differences between groups were assessed by paired Student's *t* test for normally distributed data or paired Wilcoxon matched-pairs signed-rank test for data not normally distributed. * indicates $P \leq 0.05$; # indicates $P < 0.1$.

sperm sncRNA profile also form a key part of the immediate response to acute heat challenge.

Despite harboring an altered epigenetic landscape, heat-exposed spermatozoa retained the ability to navigate the female reproductive tract and fertilize the oocyte in both an in vivo and in vitro context. Thereafter, embryos appeared to undergo a viable developmental program, such that oocytes fertilized with heat-exposed spermatozoa did not succumb to either pre- or postimplantation lethality. This cohort of embryos was, however, characterized by a significant increase in the instance of multiple hatching sites from the encircling zona pellucida. While many factors can contribute to blastocyst hatching (57), in our study this phenomenon was accompanied by a marked acceleration of early preimplantation embryo development. However, consistent with no evidentiary link between blastocyst hatching and subsequent implantation and development (58), litter sizes sired from heat and control males proved comparable. These findings nevertheless prompted us to examine gene

expression profiles in preimplantation embryos, a strategy that revealed pronounced signatures of transcriptomic dysregulation. Notably, transcriptomic profiling was conducted on 4-cell stage embryos and thus timed to shortly follow the major wave of zygotic genome activation that occurs in 2-cell stage mouse embryos (59). Such analyses therefore obfuscate the deleterious impact on embryonic gene expression being attributed to heat-induced damage to the sperm genome. This conclusion is consistent with our inability to detect an increased burden of DNA strand breaks or oxidative adducts in the fertilizing population of heat-exposed spermatozoa. It also aligns with the demonstration that the phenotype of accelerated embryo development was able to be partially recapitulated via the direct microinjection of RNAs harvested from the spermatozoa of heat-exposed males into wild-type embryos. Indeed, equivalent trends of accelerated embryo development were recorded despite the technical challenges associated with the necessity to use different mouse strains and in vitro embryo culture conditions for

these experiments (please see *Materials and Methods*). Further, while recognized as the current gold standard in substantiating the regulatory role of sperm RNA, this microinjection protocol is not without limitations. Specifically, the practice of microinjecting total sperm RNA into an oocyte that has been prefertilized with control sperm limits the ability to assess the impact of RNAs whose abundance was reduced in response to heat exposure. This may, at least in part, account for why the microinjection of RNAs harvested from heat-exposed spermatozoa did not recapitulate all observed embryo phenotypes (i.e., multiple hatching). Alternatively, additional nongenetic factors such as heat-induced modification of sperm chromatin architecture, which were not examined in this study, may also contribute to the transmission of the observed phenotypes. It should also be noted that our analysis did not extend to investigating whether microinjection of RNA from heat-exposed spermatozoa contributed to downstream effects on placental architecture or increased fetal:placental weight ratios. Nevertheless, such data implicate heat-sensitive sperm RNAs among the putative causative agents responsible for altering the trajectory of preimplantation embryonic development. These data, in turn, build on a growing body of evidence that sperm RNAs can indeed influence early embryonic gene development by virtue of their ability to regulate the stability and/or the translation of maternal/embryonic mRNA transcripts, and remodel chromatin and DNA demethylation marks (40, 45, 60).

Given that our studies were terminated prior to birth, the implications for offspring of heat-exposed fathers await further detailed investigation. However, as the end point for our analysis, pups sired by heat-exposed spermatozoa were shown to be larger than that of their control counterparts at necropsy on day 17.5 of gestation. While we cannot eliminate the possibility that the acceleration of early preimplantation embryo development and an increase in pup weight are independent events, the prospect that these phenotypes are linked to heat-sensitive changes in the sperm epigenome is given credence by multiple lines of evidence. These include the dysregulation of several 4-cell and morula embryo genes implicated in "abnormal placental morphology" and the corresponding elevation of candidate sperm sncRNAs such as *miR-127-3p*, which has been linked to regulation of fetal capillaries within the labyrinth zone during placentation (61). Accordingly, we documented changes in placental architecture such that the labyrinth zone area of pups sired by heat-exposed males was significantly increased above that of control pups. The biological significance of such changes rests with the role of the labyrinth zone as the site of nutrient exchange between the maternal and fetal blood circulations (62). Thus, previous studies have shown that an increase in labyrinth zone area and an attendant increase in placental efficiency (63, 64) is associated with an increase in fetal growth (62, 65), possibly contributing to the phenotype of larger fetuses sired by heat-exposed males. Irrespective, from a clinical context, the presentation of a large for gestational age fetus carries with it an increased risk of pregnancy and parturition complications for both mother and child (66). Beyond the immediate risk posed by delivery complications, large fetuses are also predisposed to developing a myriad of pathophysiological conditions as well as the onset of metabolic syndromes later in life (67, 68). While the etiology of increased fetal size is undeniably complex, most research to date has focused on maternal contributions to this phenomenon (68, 69). However, our study, as well as others focusing on the impact of advanced paternal age (70), raises the prospect that the periconceptual paternal environment may also exert

influence on neonatal weight. When considering the underlying mechanism of this phenomenon, previous research has suggested that aging exerts epigenetic changes in spermatozoa including methylation status and histone modifications (71). Additionally, seminal plasma composition is also now recognized as being sensitive to the paternal environment (72–76) and has been shown to influence embryonic developmental trajectory and offspring health independent of spermatozoa (77–80). While we are unable to preclude such influences, the timing of the applied heat exposure regimen and our experimental design firmly implicate stress signals encountered during posttesticular sperm transit through the epididymal environment, a stage of sperm development in which the methylome of this near-mature cell is known to be particularly stable (81). This situation contrasts that of the sperm sncRNA landscape, which we have documented to be dynamically remodeled during epididymal maturation under both physiological (43) and pathophysiological conditions (46).

Although it was beyond the scope of the present study to explore whether the alteration to miRNA/target gene expression modules documented herein may be conserved across species, it is nonetheless of interest that an accelerated rate of development has also been noted as a primary response to abiotic stressors, including heat, among model plant species. For instance, it has been shown that the cultivation of *Arabidopsis thaliana* (*Arabidopsis*) plants under an elevated temperature regimen results in the promotion of aerial tissue growth parameters (82–84). Notably, in a response that has striking parallels with that documented here, such high temperature-mediated adaptations in plant architecture have been linked with stress hormone induction (82), transcription factor expression (83), and abundance alterations in miRNA landscapes of heat-stressed *Arabidopsis* seedlings (84). Together, such data encourage speculation that these responses may form part of an evolutionary conserved molecular pathway elicited by hyperthermic stressors encountered across a phylogenetically diverse range of species among both plant and animal kingdoms.

Conclusions

In summary, here, we provide evidence that acute whole-body heat exposure designed to emulate conditions encountered during a heat wave event, alters the sncRNA profile of mouse spermatozoa leading to a downstream sequela of dysregulated embryonic gene expression, accelerated preimplantation development, aberrant blastocyst hatching, and increased fetal:placental weight ratio. Such data highlight that even a relatively modest elevation in ambient temperature can affect male reproductive function by eliciting changes to the paternal epigenome that would likely evade most traditional forms of sperm analysis (85). While recognizing the overarching importance of the testes to male reproductive health, these data nonetheless identify the acute sensitivity of posttesticular sperm development to paternal stressors and thus reinforce the broader role of epididymal transit as a critical developmental window responsible for shaping sperm function. Beyond the immediate relevance to assessing the impact of climate change on animal reproduction, such findings are also of clinical interest when considered in the context of epidemiological evidence that the human epididymis may be operating in a temperature-repressed state in modern society (17). Together, this research highlights the importance of preconception male health and provides the impetus for continued investigation into the precursory mechanisms by which hyperthermic stress impacts male fertility and ultimately offspring health.

Materials and methods

Please see *SI Appendix*, for a detailed description of the Materials and Methods.

Whole-Body Heat Exposure Regimen. All experimental protocols were approved by the University of Newcastle Animal Care and Ethics Committee (Ethics number A-2019-901). Unrestrained adult male Swiss mice (8 to 12 wk of age) were housed in cages of 4 to 5 animals and exposed to an elevated environmental temperature regimen generated via a dedicated animal intensive care unit (Lyon Technologies, Chula Vista, CA, USA), with food and water provided ad libitum. Heat exposure was performed for 7 d using a daily temperature cycle of 8 h at 35 °C (during light cycle), followed by 16 h recovery at 25 °C, and a constant humidity of 30% (*SI Appendix*, Fig. S1*A*). Control mice were also housed under identical conditions, with the sole difference being that the intensive care unit was maintained at a constant temperature of 21 °C for the duration of the exposure period (*SI Appendix*, Fig. S1*A*). Following exposure, on the morning of day 8, mice were killed via CO_2 asphyxiation. Importantly, the duration of exposure was selected to coincide with that encountered during a prolonged heat wave and with sperm transit through the epididymis. Thus, spermatozoa harvested from the cauda epididymis in preparation for functional analyses and RNA-Seq would have experienced heat load exclusively while residing in the epididymis (35). This strategy enabled discrimination of the effects attributed to the epididymal environment away from that of any upstream consequences arising during spermatogenesis in the testis.

Data, Materials, and Software Availability. Raw and processed sequencing data have been deposited in NCBI's Gene Expression Omnibus and are accessible via the following accession GSE252418 (86). All other data are included in the article and/or *SI Appendix*.

Author affiliations: [a]School of Environmental and Life Sciences, The University of Newcastle, Callaghan, NSW 2308, Australia; [b]Infertility and Reproduction Research Program, Hunter Medical Research Institute, New Lambton Heights, NSW 2305, Australia; [c]Department of Genetics Epigenetics Institute, Institute of Regenerative Medicine, University of Pennsylvania Perelman School of Medicine, Philadelphia, PA 19104; [d]Department of Pediatrics Epigenetics Institute, Institute of Regenerative Medicine, University of Pennsylvania Perelman School of Medicine, Philadelphia, PA 19104; [e]Center for Reproductive and Women's Health, University of Pennsylvania Perelman School of Medicine, Philadelphia, PA 19104; [f]Division of Neonatology, Children's Hospital of Philadelphia, Philadelphia, PA 19104; [g]Institute of Experimental Genetics, Helmholtz Zentrum München, German Research Center for Environmental Health, Neuherberg 85764, Germany; [h]German Center for Diabetes Research, Deutsche Zentrum für Diabetesforschung, Neuherberg 85764, Germany; [i]School of BioSciences Bio21 Molecular Sciences and Biotechnology Institute, Faculty of Science, University of Melbourne, Parkville, VIC 3010, Australia; [j]NSW Health Pathology, Newcastle, NSW 2300, Australia; [k]Cancer Signaling Research Group, School of Biomedical Sciences and Pharmacy, Faculty of Health and Medicine, University of Newcastle, Callaghan, NSW 2308, Australia; [l]Precision Medicine Research Program, Hunter Medical Research Institute, New Lambton Heights, NSW 2305, Australia; and [m]School of Health, University of the Sunshine Coast, Maroochydore, QLD 4558, Australia

Author contributions: N.A.T., J.E.S., J.H.M., G.N.D.I., S.D.R., E.G.B., M.D.D., A.L.E., and B.N. designed research; N.A.T., J.E.S., J.H.M., D.A.S.-B., S.P.S., I.R.B., A.L.A., S.J.S., E.N.A.S., A.T., R.T., C.C.C., A.L.E., and B.N. performed research; A.T., R.T., and C.C.C. contributed new reagents/analytic tools; N.A.T., J.E.S., J.H.M., D.A.S.-B., S.P.S., I.R.B., A.L.A., S.J.S., E.N.A.S., A.T., R.T., C.C.C., G.N.D.I., S.D.R., E.G.B., M.D.D., A.L.E., and B.N. analyzed data; B.N. and M.D.D. sourced funding; and N.A.T., J.E.S., J.H.M., D.A.S.-B., S.P.S., A.L.A., R.T., C.C.C., G.N.D.I., S.D.R., E.G.B., M.D.D., A.L.E., and B.N. wrote the paper.

1. Climate Change 2014: Synthesis Report, *Contribution of Working Groups I, II and III to the Fifth Assessment Report of the Intergovernmental Panel on Climate Change*, R. K. Pachauri, L. A. Meyer, Eds. (Intergovernmental Panel on Climate Change, Geneva, Switzerland, 2014), p. 151.
2. P. J. Robinson, On the definition of a heat wave. *J. Appl. Meteorol.* **40**, 762–775 (2001).
3. J. A. Nienaber, G. L. Hahn, T. M. Brown-Brandl, R. A. Eigenberg, "Summer heat waves–Extreme years" in *2007 ASAE Annual Meeting* (American Society of Agricultural and Biological Engineers, 2007).
4. U. Nidumolu *et al.*, Spatio-temporal modelling of heat stress and climate change implications for the Murray dairy region, Australia. *Int. J. Biometeorol.* **58**, 1095–1108 (2014).
5. V. Thompson *et al.*, The 2021 western North America heat wave among the most extreme events ever recorded globally. *Sci. Adv.* **8**, eabm6860 (2022).
6. J. Blackshaw, A. Blackshaw, Heat stress in cattle and the effect of shade on production and behaviour: A review. *Aust. J. Exp. Agric.* **34**, 285–295 (1994).
7. G. L. Hahn, Dynamic responses of cattle to thermal heat loads. *J. Anim. Sci.* **77**, 10–20 (1999).
8. G. L. Hahn, T. L. Mader, "Heat waves in relation to thermoregulation, feeding behaviour and mortality of feedlot cattle" in *Livestock Environment V, Proceedings of the Fifth International Symposium*, , R. W. Bottcher, S. J. Hoff, Eds. (St. Joseph, MI, 1997), pp. 563–571.
9. A. M. Lees, M. L. Sullivan, J. C. W. Olm, A. J. Cawdell-Smith, J. B. Gaughan, The influence of heat load on Merino sheep. 2. Body temperature, wool surface temperature and respiratory dynamics. *Anim. Prod. Sci.* **60**, 1932–1939 (2020).
10. A. M. Lees, M. L. Sullivan, J. C. W. Olm, A. J. Cawdell-Smith, J. B. Gaughan, The influence of heat load on Merino sheep. 1. Growth, performance, behaviour and climate. *Anim. Prod. Sci.* **60**, 1925–1931 (2020).
11. A. M. Lees *et al.*, The influence of heat load on Merino sheep. 3. Cytokine and biochemistry profiles. *Anim. Prod. Sci.* **60**, 1940–1948 (2020).
12. S. R. Mishra, Behavioural, physiological, neuro-endocrine and molecular responses of cattle against heat stress: An updated review. *Trop. Anim. Health Prod.* **53**, 400 (2021).
13. A. Bansal *et al.*, Heatwaves and wildfires suffocate our healthy start to life: Time to assess impact and take action. *Lancet. Planet Health* **7**, e718–e725 (2023).
14. I. Khan *et al.*, Heat stress as a barrier to successful reproduction and potential alleviation strategies in cattle. *Animals (Basel)* **13**, 2359 (2023).
15. M. L. Rhoads, Review: Reproductive consequences of whole-body adaptations of dairy cattle to heat stress. *Animal* **17**, 100847 (2023).
16. B. R. Robinson, J. K. Netherton, R. A. Ogle, M. A. Baker, Testicular heat stress, a historical perspective and two postulates for why male germ cells are heat sensitive. *Biol. Rev. Camb. Philos. Soc.* **98**, 603–622 (2023).
17. J. M. Bedford, Human spermatozoa and temperature: The elephant in the room. *Biol. Reprod.* **93**, 97 (2015).
18. J. M. Bedford, Singular features of fertilization and their impact on the male reproductive system in eutherian mammals. *Reproduction* **147**, R43–R52 (2014).
19. J. P. Kastelic, G. Rizzoto, J. Thundathil, Review: Testicular vascular cone development and its association with scrotal thermoregulation, semen quality and sperm production in bulls. *Animal* **12**, s133–s141 (2018).
20. G. Rizzoto, J. P. Kastelic, A new paradigm regarding testicular thermoregulation in ruminants? *Theriogenology* **147**, 166–175 (2020).
21. R. A. Aldahhan, P. G. Stanton, Heat stress response of somatic cells in the testis. *Mol. Cell Endocrinol.* **527**, 111216 (2021).
22. D. Durairajanayagam, A. Agarwal, C. Ong, Causes, effects and molecular mechanisms of testicular heat stress. *Reprod. Biomed. Online* **30**, 14–27 (2015).
23. T. R. Hamilton *et al.*, Evaluation of lasting effects of heat stress on sperm profile and oxidative status of ram semen and epididymal sperm. *Oxid. Med. Cell Longev.* **2016**, 1687657 (2016).
24. B. J. Houston *et al.*, Heat exposure induces oxidative stress and DNA damage in the male germ line. *Biol. Reprod.* **98**, 593–606 (2018).
25. Y. X. Liu, Temperature control of spermatogenesis and prospect of male contraception. *Front. Biosci. (Schol Ed)* **2**, 730–755 (2010).
26. J. J. Parrish *et al.*, Scrotal insulation and sperm production in the boar. *Mol. Reprod. Dev.* **84**, 969–978 (2017).
27. M. Perez-Crespo, B. Pintado, A. Gutierrez-Adan, Scrotal heat stress effects on sperm viability, sperm DNA integrity, and the offspring sex ratio in mice. *Mol. Reprod. Dev.* **75**, 40–47 (2008).
28. M. B. Rahman, K. Schellander, N. L. Luceno, A. Van Soom, Heat stress responses in spermatozoa: Mechanisms and consequences for cattle fertility. *Theriogenology* **113**, 102–112 (2018).
29. G. Rizzoto, G. Boe-Hansen, C. Klein, J. C. Thundathil, J. P. Kastelic, Acute mild heat stress alters gene expression in testes and reduces sperm quality in mice. *Theriogenology* **158**, 375–381 (2020).
30. G. R. Pereira *et al.*, Effect of scrotal insulation on sperm quality and seminal plasma proteome of Brangus bulls. *Theriogenology* **144**, 194–203 (2020).
31. G. B. Boe-Hansen *et al.*, Effects of increased scrotal temperature on semen quality and seminal plasma proteins in Brahman bulls. *Mol. Reprod. Dev.* **87**, 574–597 (2020).
32. A. C. Lucio *et al.*, Selected sperm traits are simultaneously altered after scrotal heat stress and play specific roles in in vitro fertilization and embryonic development. *Theriogenology* **86**, 924–933 (2016).
33. D. R. Rocha *et al.*, Effect of increased testicular temperature on seminal plasma proteome of the ram. *Theriogenology* **84**, 1291–1305 (2015).
34. H. Henning *et al.*, Effect of short-term scrotal hyperthermia on spermatological parameters, testicular blood flow and gonadal tissue in dogs. *Reprod. Domest. Anim.* **49**, 145–157 (2014).
35. B. Nixon *et al.*, Molecular insights into the divergence and diversity of post-testicular maturation strategies. *Mol. Cell Endocrinol.* **517**, 110955 (2020).
36. W. Zhou, G. N. De Iuliis, M. D. Dun, B. Nixon, Characteristics of the epididymal luminal environment responsible for sperm maturation and storage. *Front. Endocrinol. (Lausanne)* **9**, 59 (2018).
37. B. Nixon *et al.*, Profiling of epididymal small non-protein-coding RNAs. *Andrology* **7**, 669–680 (2019).
38. N. A. Trigg, A. L. Eamens, B. Nixon, The contribution of epididymosomes to the sperm small RNA profile. *Reproduction* **157**, R209–R223 (2019).
39. N. A. Trigg *et al.*, Quantitative proteomic dataset of mouse caput epididymal epithelial cells exposed to acrylamide in vivo. *Data Brief* **42**, 108032 (2022).
40. C. C. Conine, F. Sun, L. Song, J. A. Rivera-Pérez, O. J. Rando, Small RNAs gained during epididymal transit of sperm are essential for embryonic development in Mice. *Dev. Cell* **46**, 470–480.e3 (2018).
41. C. C. Conine, F. Sun, L. Song, J. A. Rivera-Perez, O. J. Rando, MicroRNAs absent in caput sperm are required for normal embryonic development. *Dev. Cell* **50**, 7–8 (2019).
42. K. Hutcheon *et al.*, Analysis of the small non-protein-coding RNA profile of mouse spermatozoa reveals specific enrichment of piRNAs within mature spermatozoa. *RNA Biol.* **14**, 1776–1790 (2017).
43. B. Nixon *et al.*, The microRNA signature of mouse spermatozoa is substantially modified during epididymal maturation. *Biol. Reprod.* **93**, 91 (2015).

44. U. Sharma et al., Small RNAs are trafficked from the epididymis to developing mammalian sperm. Dev. Cell 46, 481–494.e6 (2018).

45. U. Sharma et al., Biogenesis and function of tRNA fragments during sperm maturation and fertilization in mammals. Science 351, 391–396 (2016).

46. N. A. Trigg et al., Acrylamide modulates the mouse epididymal proteome to drive alterations in the sperm small non-coding RNA profile and dysregulate embryo development. Cell Rep. 37, 109787 (2021).

47. S. Yuan et al., Sperm-borne miRNAs and endo-siRNAs are important for fertilization and preimplantation embryonic development. Development (Cambridge, England) 143, 635–647 (2016).

48. Y. Chen, X. Wang, miRDB: An online database for prediction of functional microRNA targets. Nucleic Acids Res. 48, D127–D131 (2020).

49. Intergovernmental Panel on Climate Change, Climate Change 2022: Impacts, Adaptation, and Vulnerability, Contribution of Working Group II to the Sixth Assessment Report of the Intergovernmental Panel on Climate Change, H.-O. Pörtner et al., Eds. (Cambridge University Press, Cambridge, United Kingdom and New York, NY, 2022), 3056 p. DOI: 10.1017/9781009325844.

50. A. M. Shahat, G. Rizzoto, J. P. Kastelic, Amelioration of heat stress-induced damage to testes and sperm quality. Theriogenology 158, 84–96 (2020).

51. L. De Toni, F. Finocchi, K. Jawich, A. Ferlin, Global warming and testis function: A challenging crosstalk in an equally challenging environmental scenario. Front. Cell Dev. Biol. 10, 1104326 (2022).

52. E. R. James et al., The role of the epididymis and the contribution of epididymosomes to mammalian reproduction. Int. J. Mol. Sci. 21, 5377 (2020).

53. H. Rodriguez-Martinez, J. Roca, M. Alvarez-Rodriguez, C. A. Martinez-Serrano, How does the boar epididymis regulate the emission of fertile spermatozoa? Anim. Reprod. Sci. 246, 106829 (2022).

54. D. A. Skerrett-Byrne et al., Global profiling of the proteomic changes associated with the post-testicular maturation of mouse spermatozoa. Cell Rep. 41, 111655 (2022).

55. N. A. Trigg, A. L. Eamens, B. Nixon, The contribution of epididymosomes to the sperm small RNA profile. Reproduction 157, R209 (2019).

56. K. Gapp et al., Implication of sperm RNAs in transgenerational inheritance of the effects of early trauma in mice. Nat. Neurosci. 17, 667–669 (2014).

57. M. Ma et al., Effect of blastocyst development on hatching and embryo implantation. Theriogenology 214, 66–72 (2024).

58. Y. P. Cheon et al., Role of actin filaments in the hatching process of mouse blastocyst. Zygote 7, 123–129 (1999).

59. C. Yao, W. Zhang, L. Shuai, The first cell fate decision in pre-implantation mouse embryos. Cell Regen. 8, 51–57 (2019).

60. A. B. Rodgers, C. P. Morgan, N. A. Leu, T. L. Bale, Transgenerational epigenetic programming via sperm microRNA recapitulates effects of paternal stress. Proc. Natl. Acad. Sci. U.S.A. 112, 13699–13704 (2015).

61. M. Ito et al., A trans-homologue interaction between reciprocally imprinted miR-127 and Rtl1 regulates placenta development. Development 142, 2425–2430 (2015).

62. L. Woods, V. Perez-Garcia, M. Hemberger, Regulation of placental development and its impact on fetal growth-new insights from mouse models. Front. Endocrinol. (Lausanne) 9, 570 (2018).

63. A. L. Fowden, A. N. Sferruzzi-Perri, P. M. Coan, M. Constancia, G. J. Burton, Placental efficiency and adaptation: Endocrine regulation. J. Physiol. 587, 3459–3472 (2009).

64. C. E. Hayward et al., Placental Adaptation: What can we learn from birthweight:Placental weight ratio?. Front. Physiol. 7, 28 (2016).

65. O. Cisse et al., Mild gestational hyperglycemia in rat induces fetal overgrowth and modulates placental growth factors and nutrient transporters expression. PLoS One 8, e64251 (2013).

66. National Guideline Alliance (UK), Induction of labour for suspected fetal macrosomia, Inducing labour: Evidence review A (NICE Guideline, No. 207, National Institute for Health and Care Excellence (NICE), London, United Kingdom, 2021). https://www.ncbi.nlm.nih.gov/books/NBK579534/.

67. Macrosomia: ACOG Practice Bulletin, Number 216. Obstet. Gynecol. 135, e18–e35 (2020).

68. F. Fang et al., Risk factors for recurrent macrosomia and child outcomes. World J. Pediatr. 15, 289–296 (2019).

69. A. Mohammadbeigi et al., Fetal macrosomia: Risk factors, maternal, and perinatal outcome. Ann. Med. Health Sci. Res. 3, 546–550 (2013).

70. Y. H. Chung, I. S. Hwang, G. Jung, H. S. Ko, Advanced parental age is an independent risk factor for term low birth weight and macrosomia. Medicine (Baltimore) 101, e29846 (2022).

71. K. Xie et al., Epigenetic alterations in longevity regulators, reduced life span, and exacerbated aging-related pathology in old father offspring mice. Proc. Natl. Acad. Sci. U.S.A. 115, E2348–E2357 (2018).

72. N. K. Binder, J. R. Sheedy, N. J. Hannan, D. K. Gardner, Male obesity is associated with changed spermatozoa Cox4i1 mRNA level and altered seminal vesicle fluid composition in a mouse model. Mol. Hum. Reprod. 21, 424–434 (2015).

73. A. B. Javurek et al., Consumption of a high-fat diet alters the seminal fluid and gut microbiomes in male mice. Reprod. Fertil. Dev. 29, 1602–1612 (2017).

74. C. S. Rosenfeld et al., Seminal fluid metabolome and epididymal changes after antibiotic treatment in mice. Reproduction 156, 1–10 (2018).

75. J. E. Schjenken et al., High-fat diet alters male seminal plasma composition to impair female immune adaptation for pregnancy in mice. Endocrinology 162, bqab123 (2021).

76. D. A. Skerrett-Byrne et al., Proteomic dissection of the impact of environmental exposures on mouse seminal vesicle function. Mol. Cell Proteomics 20, 100107 (2021).

77. J. J. Bromfield et al., Maternal tract factors contribute to paternal seminal fluid impact on metabolic phenotype in offspring. Proc. Natl. Acad. Sci. U.S.A. 111, 2200–2205 (2014).

78. M. Lassi et al., Disruption of paternal circadian rhythm affects metabolic health in male offspring via nongerm cell factors. Sci. Adv. 7, eabg6424 (2021).

79. H. L. Morgan et al., Paternal low protein diet perturbs inter-generational metabolic homeostasis in a tissue-specific manner in mice. Commun. Biol. 5, 929 (2022).

80. A. J. Watkins et al., Paternal diet programs offspring health through sperm- and seminal plasma-specific pathways in mice. Proc. Natl. Acad. Sci. U.S.A. 115, 10064–10069 (2018).

81. C. Galan et al., Stability of the cytosine methylome during post-testicular sperm maturation in mouse. PLoS Genet. 17, e1009416 (2021).

82. W. M. Gray, A. Ostin, G. Sandberg, C. P. Romano, M. Estelle, High temperature promotes auxin-mediated hypocotyl elongation in Arabidopsis. Proc. Natl. Acad. Sci. U.S.A. 95, 7197–7202 (1998).

83. M. A. Koini et al., High temperature-mediated adaptations in plant architecture require the bHLH transcription factor PIF4. Curr. Biol. 19, 408–413 (2009).

84. J. L. Pegler, J. M. J. Oultram, C. P. L. Grof, A. L. Eamens, Profiling the abiotic stress responsive microRNA Landscape of Arabidopsis thaliana. Plants (Basel) 8, 58 (2019).

85. B. Nixon et al., New horizons in human sperm selection for assisted reproduction. Front. Endocrinol. (Lausanne) 14, 1145533 (2023).

86. N. A. Trigg et al., Subchronic elevation in ambient temperature drives alterations to the sperm epigenome and accelerates early embryonic development in mice. NCBI Gene Expression Omnibus. https://www.ncbi.nlm.nih.gov/geo/query/acc.cgi?acc=GSE252418. Deposited 3 January 2024.